Electrochimica Acta 140 (2014) 232–237

Contents lists available at ScienceDirect

Electrochimica Acta

journal homepage: www.elsevier.com/locate/electacta

First-principles studies of lithium storage in reduced graphite oxide

C.B. Robledo [a], M. Otero [a], G. Luque [a], O. Cámara [a], D. Barraco [b], M.I. Rojas [a], E.P.M. Leiva [a,*]

[a] INFIQC, Departamento de Matemática y Física, Facultad de Ciencias Químicas, Universidad Nacional de Córdoba, Ciudad Universitaria, 5000 Córdoba, Argentina

[b] IFEG, Facultad de Matemática Astronomía y Física, Universidad Nacional de Córdoba, Ciudad Universitaria, 5000 Córdoba. Argentina

ARTICLE INFO

Article history:
Received 15 December 2013
Received in revised form 7 July 2014
Accepted 8 July 2014
Available online 16 July 2014

Keywords:
Lithium storage
reduced graphite oxide
Density Functional Theory.

ABSTRACT

The present work performs a first-principles study of the lithiation of graphite oxides with low oxygen content, which resemble reduced graphite oxide materials. The chemical nature of the Li structure formed is analysed, leading to the conclusion that the nature of lithium binding in these materials is completely different from that observed in pristine graphite. The stability of the lithium structures formed under different loadings is studied, with the finding that the lithiation potentials predicted are within the ranges of the values observed experimentally.

1. Introduction

Rechargeable Li-ion batteries (LIBs) appear nowadays as promissory energy storage media for many applications, ranging from portable electronic devices up to electric vehicles (EV). However, for the more demanding applications uses such as EV and load-levelling applications, the challenge that remains is to improve the energy and power densities without increasing weight [1–5]. Therefore, a large amount of effort is being undertaken in the scientific and engineering community in the development of new electrode materials for this type of batteries.

Carbonaceous materials present a lot of advantages due to their excellent properties such as good thermal and electronic conductivity and great surface area, among others. In summary, these properties make them attractive materials for innumerable applications, particularly in the field of energy carriers, like hydrogen storage and electrochemical systems. Among the latter, the commercial anodes of Li-ion batteries are a typical example. In fact, graphite is the most commonly used carbon material in the manufacture of the anodes of Li-ion batteries, allowing Li ions to be stored up to a LiC_6 stoichiometry, which implies a maximum theoretical capacity of 372 mAh g^{-1} [6]. Recently, materials based on carbon nanostructures such as nanotubes [7–9] and oxidized graphene nanoribbons [10] obtained by unzipping of the carbon nanotubes [11], have been shown to outperform the Li-ion storage capacity of ordinary graphitic materials. Similarly, graphene nanosheets have been found to yield a capacity of 460 mAh g^{-1} for 100 cycles work [12] and in the case of disordered graphene nanosheets the reported reversible capacity has been even larger, ranging between 794 and 1054 mAh g^{-1} [13]. Oxidized graphene nanoribbons have shown an initial capacity of 1400 mAh g^{-1} and a reversible capacity of 800 mAh g^{-1} [10]. Something similar happens with graphite oxide with different degrees of oxidation [14] and reduced graphite oxide [15]. However, up to date storage in oxidized graphitic systems has received relatively little attention in the theoretical field [16] in comparison with studies of pristine graphitic materials [17–21]. On the other hand, highly porous structures composed of carbon nanotubes or graphite oxide can be decorated with different metals (Ti, Ni, Co, Mn, V) to promote the intercalation of lithium. These experiments also indicate that it would be possible to increase the maximum ratio of 1:6 (Li:C) found for graphite. Thus, theoretical advances in the understanding of the absorption/desorption mechanism of Li^+ ions for the new carbon materials are critical to increase the actual performance and to acquire knowledge in the experimental limitations of the carbonaceous anode materials.

In the present work we investigate lithiation of mildly oxidized graphitic nanostructures, sometimes referred as reduced graphite oxide (RGO) [16], by means of first-principles calculations. We analyse the chemical nature of the modified carbonaceous-Li structures and consider the stability of them under different Li-loadings.

1.1. Methodology

1.1.1. Calculation details

All DFT calculations were performed using the Quantum Espresso package [22] with Van der Waals interactions. The

* Corresponding author.
E-mail addresses: eze_leiva@yahoo.com.ar, eleiva@fcq.unc.edu.ar (E.P.M. Leiva).

http://dx.doi.org/10.1016/j.electacta.2014.07.013
0013-4686/

Kohn-Sham orbitals and charge density were expanded in plane-waves basis sets up to a kinetic energy cutoff of 30 and 300 Ry for all atoms respectively. Ultra soft pseudopotentials were employed with the Perdew-Wang approximation for exchange and correlation in the PW91 functional [23–25]. The application of this functional to a system closely related to the present one has been validated in a very recent article [26]. The Brillouin zone was sampled with $3 \times 3 \times 1$ irreducible Monkhorst-Pack k-point grid [27]. The convergence threshold for the total energy at each electronic calculations was set to 1×10^{-6} Ry. Geometry optimizations were performed employing the Broyden-Fletcher-Goldfarb-Shanno (BFGS) algorithm (for stress minimization) and total forces acting on each ion were minimized to reach less than 1×10^{-3} Ry/a.u. by movement of the ionic positions.

1.2. Model for reduced graphite oxide

The RGO structures were represented by means of a unit cell made of two carbon sheets of 32 C atoms each, stacked in an AB arrangement as in the case of graphite. The unit cell was tetragonal $(0.986 \times 0.854 \times c)\ nm^3$ with periodic boundary conditions in the x,y,z coordinates and the c value was equal to twice the interlayer distance (d).

In order to represent the RGO structures, different amounts of epoxy (-O-) and hydroxyl (-OH) groups were randomly arranged to represent amorphous oxides, as proposed by Liu *et al.* [28]. In the present work we consider an amorphous oxide with low oxygen content and in the ratio of 2:1 between (OH:O) functional groups, which is within the [1.06:3.25] interval of oxides most frequently observed in the experiments. The unit cell used to get the results presented here is shown in Fig. 1.

We have performed previously a complete study of the properties of this system. It is pertinent here a comment concerning the stability of RGO structures with respect to exfoliation, so that we shortly revisit here the results of our previous work. While the exfoliation energy for pristine graphite layers was 0.31 J/m^2, the result for the present RGO structure yielded the same value within the calculation accuracy. For structures with larger oxygen content, the exfoliation energy increased up to 1.89 J/m^2 [29]. The reason why graphite oxides dissolve relatively easily in aqueous solutions is to be found in the strong interaction of the oxidized surface species with the solvent via hydrogen bonds. This problem will be probably reduced in the case of nonpolar solvents.

1.3. The lithiation potential and specific capacity

We denominate with the term *lithiation* the process that occurs when lithium is inserted/intercalated in the active anode material, in the present case reduced graphite oxide. The lithiation potential, V_{lit}, can be represented by the following equation, as has been employed to characterize electrode materials by other authors [30,31]:

$$V_{lit} = -\frac{\Delta G_f}{z \cdot F} \tag{1}$$

where z is the number of electrons involved in the electrochemical reaction, here 1, and F is the Faraday constant, 96485 C/mol. The change in the formation Gibb's free energy is:

$$\Delta G_f = \Delta E_f + P\Delta V_f - T\Delta S_f \tag{2}$$

where, ΔE_f, ΔV_f and $\Delta S_f$are the internal energy change, the volume change and the entropy change of formation, respectively. P and T are the pressure and absolute temperature, respectively. Equation (1) can be straightforwardly deduced from a thermodynamic cycle where a lithium cation is taken under equilibrium conditions from a reference pure Li electrode material into a working electrode made of the material under consideration. Since the term $P\Delta V_f$ is in the order of 10^{-5} eV and the entropy term is in the order of the thermal energy, k_BT (that is, Boltzmann constant multiplied by the temperature, which amounts about 25 meV at 298 K), the entropy and pressure terms can be neglected in comparison with the internal energy, which is of the order of 1 to 4 eV for the different systems and we can approximate the change in the formation Gibb's energy to the internal energy $\Delta G_f \simeq \Delta E_f$ obtained from DFT calculations. The internal energy of the Li-graphite oxide compound is defined as follows:

$$\Delta E_f = E_{Li_xGO} - E_{GO} - xE_{Li} \tag{3}$$

where E_{Li_xGO} is the total energy of the Li_xGO structure with x Li atoms intercalated, E_{GO} is the total energy of a particular GO structure and E_{Li} is the total energy of a single Li atom in the elemental body-centered cubic Li structure. If the energies are expressed in electron volts, the potential in volts of the Li_xGO structure vs. Li^+/Li^0 as a function of lithium content can be obtained from [16]:

$$V_{Lit} = \frac{-\Delta E_f}{x \cdot e_0} \tag{4}$$

where $e_0$is the elementary charge. The theoretical capacity of the electrodes and also that of the total battery cell is determined by the amount of active material in it. It is expressed as the total quantity of electric charge involved in the complete electrochemical reaction of the electrode material. The specific Capacity is defined as [4]:

$$C = \frac{zF}{atomic\ weight} \tag{5}$$

where atomic weight is the weight of the Li_xGO structure.

2. Results and Discussion

2.1. Structural and Electronic properties of lithium absorbed in RGO

Due to their relatively low oxygen content, the RGO structures considered here present different regions, some oxidized and others resembling the pristine graphite structure. While in the latter case the carbon atoms show local sp^2 hybridization, in the former there is a change to sp^3 hybridization producing a corrugation effect in the carbon layers. We have thus considered two possibilities for the lithiation process of these structures: *a)* The Li atom is absorbed preferentially in the functionalized region (named as "Li-O") and *b)* The Li atom is absorbed in the area far away from the functionalized groups (named as "Li-C"). In *a*, the resulting lithiation potential as calculated according to equation (4) is 1.12 V and in *b* it is 0.13 V. It is remarkable that for the structure where de Li atom is near the non-functionalized section, the lithiation potential is very similar to the intercalation potential of Li in pristine graphite, as it is found in experiments [32], while for the Li-O structure the potential is much higher. In order to determine the relative stability of the different structures when more lithium ions are introduced in the RGO structure, we calculated the binding energy (E_b) per Li atom as follows:

$$E_b = \frac{E_{Li_xGO} - E_{GO} - xE_{Li,vac}}{x} \tag{6}$$

where $E_{Li,vac}$ is the total energy of a single Li atom in vacuum. The Li atom presented a binding energy of −1.60 eV in the Li-C structure and −2.59 eV in the Li-O structure. This means that absorption of the Li atom is much more favourable close to the oxygen functional groups than near the carbon atoms in the pristine graphite. To elucidate the chemical nature of this phenomenon, we calculated the electronic density differences between the electron densities of the

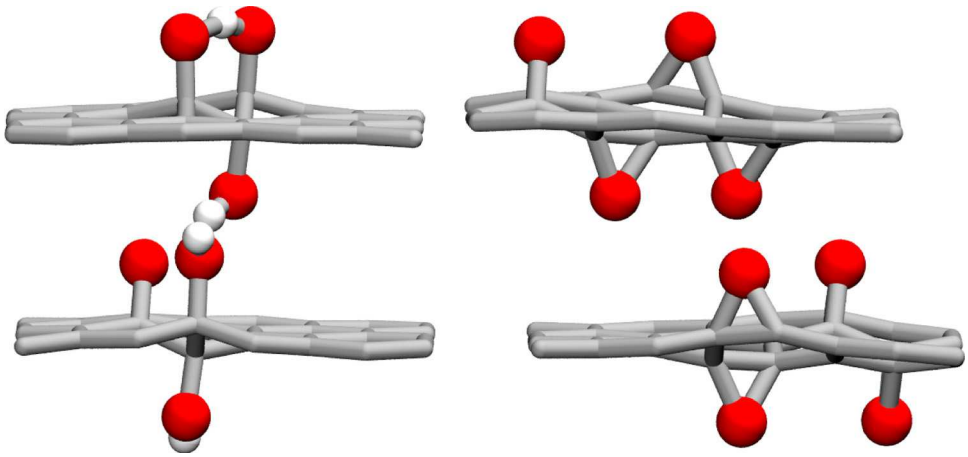

Fig. 1. (Left) Unit cell of the system used to emulate reduced graphite oxide. (Right) Unit cell used to emulate strongly oxidized graphite oxide, with epoxy groups. Grey: C-lattice; red spheres: O atoms; white spheres: H atoms.

RGO structure with a Li atom (ρ_{Li-RGO}) and those of the separated RGO (ρ_{RGO}) and Li atom (ρ_{Li}), at the optimized positions:

$$\Delta\rho = \rho_{Li-RGO} - \rho_{RGO} - \rho_{Li} \quad (7)$$

The results obtained for both structures can be observed on the left of Fig. 2 and Fig. 3. In the case of the Li-C structure, it is found that the electronic density sitting on the Li atom has moved to the bonding region between the lithium atom and the carbon rings confining it. Thus, the electronic difference plot takes the shape of a depletion donut limited above and below by two squeezed accumulation clouds. The electronic density at the C-C bonds is found to decrease, especially for those C atoms neighbouring the Li atom, as has been observed by *Valencia et al.* [17] for a Li atom absorbed onto pristine graphite. The shape of the electronic density difference in the bonding region suggests an increased population of p_z-like graphite orbitals. In fact, alkali cations in bare contact with aromatic rings have been found to display a relatively strong non-covalent bond referred to as the cation-π interaction [33]. The electronic density distribution found in this case, suggests that such a mechanism is being followed in the bonding of Li with the substrate. The ionic character of the bonding is reflected by the clear separation between carbon and lithium states in the projected electronic density of states shown on the right of Fig. 2. On the other hand, in the Li-O case, the electronic density difference plots are quite different from the previous case. Here we can observe that depletion of charge is being held near the lithium atom and at the oxygen atoms. A concentration of electronic charge is found in between these atoms. This indicates a rather covalent bond being formed between Li and O. This may be the reason for the larger binding energy of the Li atom (about 1 eV) as compared with that observed for the Li-C structure. The different nature of the binding is also evident in the projected density of states, shown on the right of Fig. 3. A meaningful contribution of the oxygen p-PDOS is found in the energy region corresponding to the lithium 2s-PDOS. Comparison of the low-energy laying oxygen-pPDOS (between -25 eV and -20 eV) with and without lithium (not shown here) indicates that these low-laying oxygen p-orbitals are stabilized by the presence of lithium in a value of about one eV. This also points to a strong interaction between lithium and the oxygen species of graphite oxide.

2.2. Simulated galvanostatic charge curve for RGO as active anode material

To emulate the charging process of the RGO material, we propose two different mechanisms possible, which are schematized in Fig. 4. The mechanism denoted A is called “alternated”, since the first lithium atom is stored in one layer of graphite, the second in the adjacent layer, the third one again in the first layer and so on. The B mechanism is denominated a “layered” one, where a layer

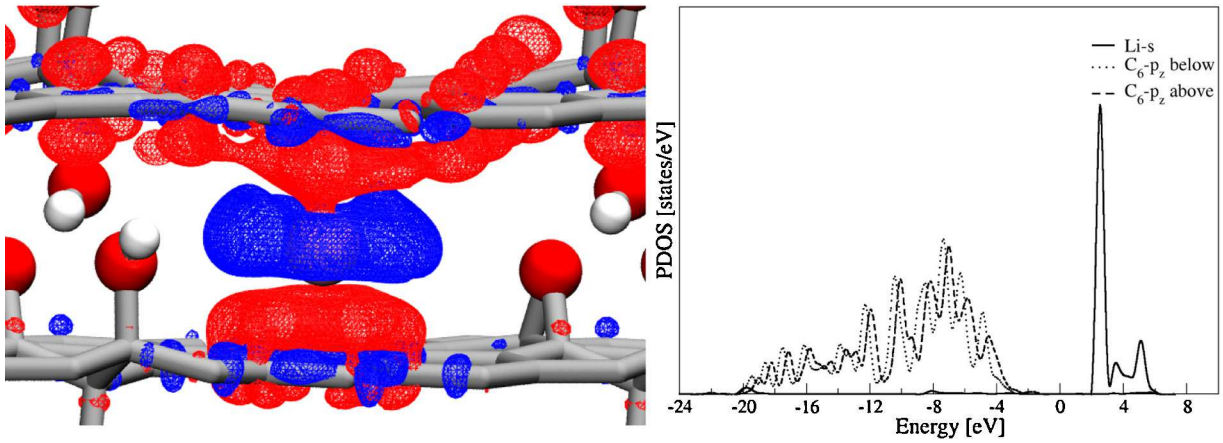

Fig. 2. Electronic density difference plots (left) due to incorporation of a Li atom in RGO at a site far from the oxygen functional groups. The isosurfaces shown correspond to a value of 0.001 e/Å^3. Red and blue colours indicate electronic charge accumulation and depletion, respectively. Grey: C-lattice; red spheres: O atoms; pink sphere: Li atom; white spheres: H atoms. The right panel shows the p_z-orbital projected density of states (PDOS) for the carbon atoms defining hexagonal rings closest to the lithium atom, one below and another one above it. The s- PDOS for the Li atom is also shown.

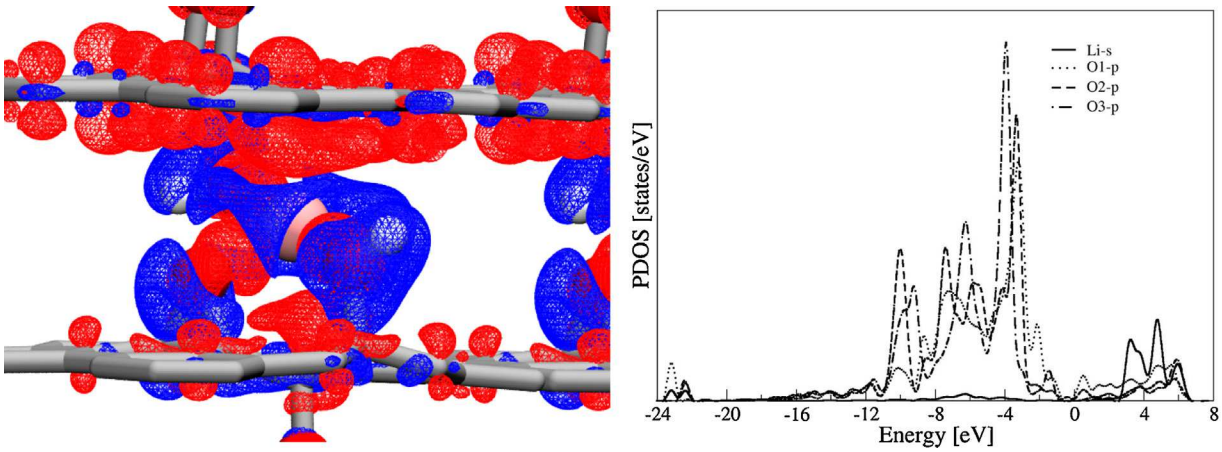

Fig. 3. Electronic density difference plots due to the incorporation of a Li atom in RGO at a site close to epoxy and hydroxyl groups. The isosurfaces shown correspond to a value of 0.001 e/Å^3. Red and blue colours indicate space charge accumulation and depletion, respectively. Grey: C-lattice; red sphere: O atoms; pink sphere: Li; white spheres: H atoms. The right panel shows the p-orbital projected density of states (PDOS) for the oxygen atoms closer to the lithium atom. The s-orbital PDOS for the Li atom is also shown. The number after the oxygen symbol indicates the order of proximity to the lithium atom.

is completely filled with Li atoms before another one starts to be filled. The later resembles the filling process in bulk graphite. We have added Li atoms consecutively following both mechanisms and calculated the average insertion potential and the specific capacity for each one. In this way, we obtained the charging curves presented in Fig. 5. It is interesting to observe that regardless the mechanism considered, there is a spreading in the lithiation potential of about one volt. This is qualitatively, and in part quantitatively, in agreement with experiments of lithium insertion from graphene oxide materials and related, where a linear voltage/capacity charging region, absent in pure graphite, is observed between 0.25 V and 1.5 V vs Li^+/Li^0. Similar results have been obtained with electrodes prepared from reduced graphene oxides [15]. In both mechanisms at approximately 200 mAh g^{-1} there is a kink in the potential. This is due to the reaction of the lithium atoms with the oxygen groups, forming lithium-oxygen species that loosen the HO-graphite bond. Thus at high loadings of lithium, chemical reactions seem to occur in these materials, which will traduce in a non-reversible capacity in the discharge process.

From the simulated galvanostatic charge curves presented above, we can conclude that the incorporation of lithium in the present type of materials takes place at potentials lower than 1 V (vs. Li^+/Li^0). In a real system, this would eventually lead to the decomposition of the solvent (for example mixed alkyl carbonates), thus leading to the formation of the Solid Electrolyte Interface (SEI) as previously discussed in the review by D. Aurbach et al. [1]. We think that the formation of the SEI would probably be easier in RGO than in graphite, since the surface would be more oxidized, containing highly reactive sites for the formation of SEI. However, the study we have presented here is relevant for the bulk material. Addressing surface phenomena related to lithium intercalation in these materials deserves further theoretical research work.

2.3. Absorption of lithium in strongly oxidized environments

The previous discussion was mainly centred on the absorption of lithium atoms in a mildly oxidized graphite environment (mixed -OH and -O- species). In order to evaluate the influence of a more strongly oxidized carbon environment, we performed calculations where all the functional groups are epoxy ones. The unit cell of this

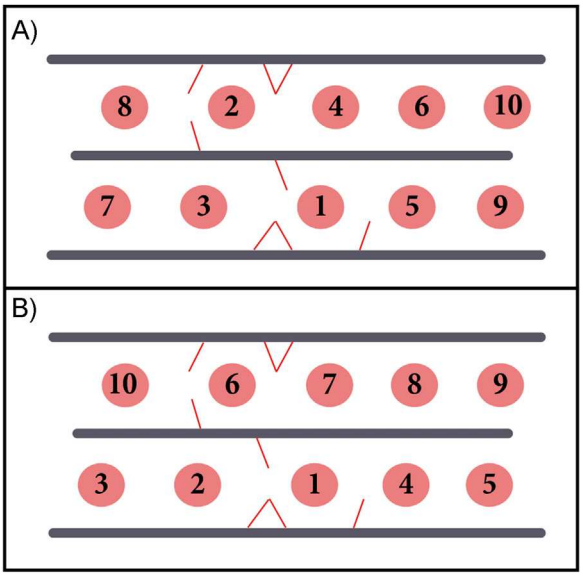

Fig. 4. Schematic mechanisms proposed for filling the reduced graphite oxide model used in the present work. A) "alternated mechanism" and B) "layered mechanism". The numbers indicate the order of the sequence in which the Li atoms are inserted. The grey lines represent the C-lattice, the pink spheres the Li atoms and the red lines the oxygen functional groups present in RGO.

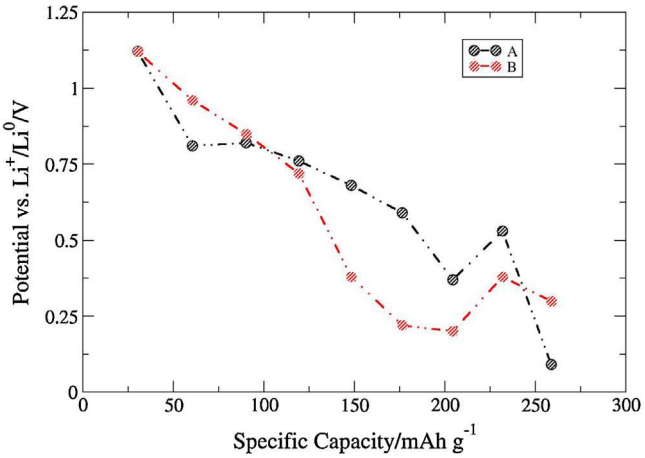

Fig. 5. Simulated galvanostatic charge curve of RGO as active anode material for lithium ion batteries. The blue line represent the proposed "alternated" and the red one the "layered" mechanisms as described in the text and Fig. 4.

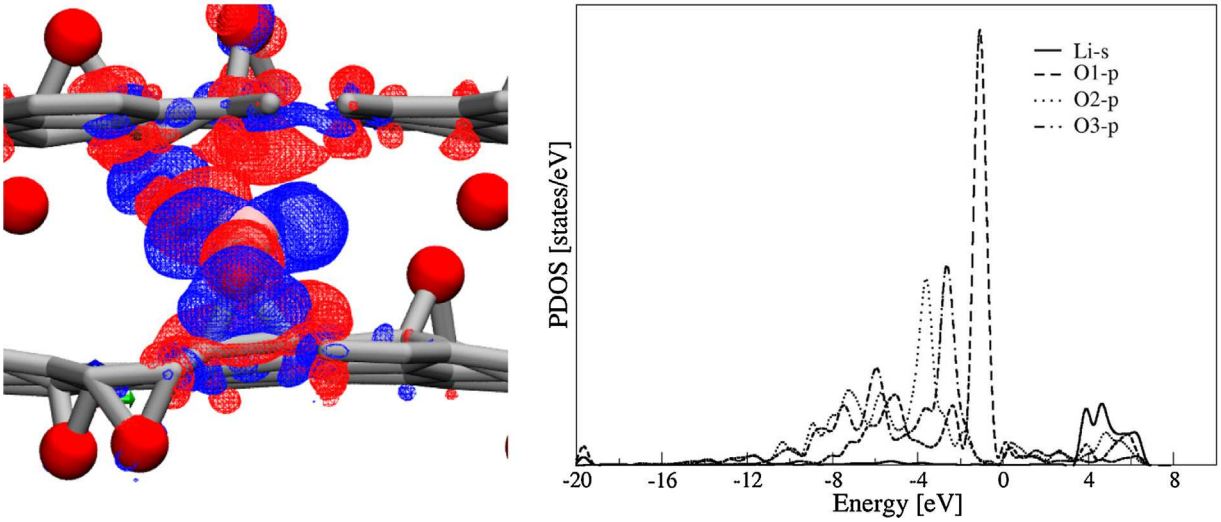

Fig. 6. Electronic density difference plots due to the incorporation of a Li atom in RGO-epoxi. The isosurfaces shown correspond to a value of 0.001 e/Å^3. Red and blue colours indicate space charge accumulation and depletion, respectively. Grey: C-lattice; red sphere: O atoms; pink sphere: Li; white spheres: H atoms. The right panel shows the p-orbital projected density of states (PDOS) for the oxygen atoms closer to the lithium atom. The s-orbital PDOS for the Li atom is also shown. The number after the oxygen symbol indicates the order of proximity to the lithium atom.

system after energy minimization is shown in Fig. 1 (right). The lithiation potential of such structure results in 2.35 V, indicating that increased oxidation of the system results in a stronger binding (and thus an increased lithiation potential) of the system. Thus, the presence of -O- species may be responsible for lithium absorption at very high potentials in graphite oxides. The differential electronic density plots, shown on the left of Fig. 6, show a concentration of electronic density between the oxygen and lithium atoms, being the carbon network only slightly affected by the formation of the new bond. While the picture given by the p-DOS on the right of Fig. 6 is qualitatively similar to that of RGO, it is found that the gap between oxygen and lithium states is decreased, with an increase of the density of states at the Fermi level. This is also an indication of a stronger interaction between lithium and the oxygen atoms.

3. Conclusions

In the present work, we have undertaken first steps towards the understanding of the interaction between lithium and a carbonaceous host material, which is made of a slightly oxidized graphitic structure. These studies were carried out in polyatomic extended systems. These first studies show that the binding of the lithium species in these materials is completely different from that observed in pristine graphite. The stability of the different lithium structures formed in these materials indicates that the lithiation potentials should be higher than those of pristine carbonaceous materials. A systematic study of similar systems with different degrees of oxidation is required to compare with experimental results of the literature, which have been obtained with a wide variety of degrees of oxidation of the graphitic substrate.

Acknowledgments

This work was supported by PID 2011-0070, PIP 11420090100066 and 11220110100992 CONICET, FONCYT PICT-2012-2324, SECyT Universidad Nacional de Córdoba, CCAD-UNC and GPGPU Computing Group. C. Robledo and M. Otero wish to thank CONICET for a doctoral fellowship.

References

[1] V. Etacheri, R. Marom, R. Elazari, G. Salitra, D. Aurbach, Challenges in the development of advanced Li-ion batteries: a review, Energy Environ. Sci. 4 (2011) 3243.
[2] K.E. Aifantis, S.A. Hackney, R.V. Kumar, High Energy Density Lithium Batteries, Wiley-VCH, Germany, 2010.
[3] J. Tarascon, N. Recham, M. Armand, J. Chotard, P. Barpanda, W. Walker, L. Dupont, Hunting for better Li-based electrode materials via low temperature inorganic synthesis, Chem. Mater. 22 (2010) 724.
[4] D. Linden, T.B. Reddy, Handbook of Batteries, McGraw-Hill, USA, 2002.
[5] Lithium Mobile Power: Advances in Lithium Battery Technologies for Mobile Applications, Knowledge Foundation, The Knowledge Press, Inc., USA, MA, 2009.
[6] D. Guerard, A. Herold, Intercalation of lithium into graphite and other carbons, Carbon 13 (1975) 337.
[7] V. Meunier, J. Kephart, C. Roland, J. Bernholc, Ab initio investigations of lithium diffusion in carbon nanotube systems, Phys. Rev. Lett. 88 (2002) 075506.
[8] B. Gao, C. Bower, J.D. Lorentzen, L. Fleming, A. Kleinhammes, X.P. Tang, L.E. McNeil, Y. Wu, O. Zhou, Enhanced saturation lithium composition in ball-milled single-walled carbon nanotubes, Chem. Phys. Lett. 327 (2000) 69.
[9] E. Yoo, J. Kim, E. Hosono, H. Zhou, T. Kudo, I. Honma, Large reversible Li storage of graphene nanosheet families for use in rechargeable lithium ion batteries, Nano Lett. 8 (2008) 2277.
[10] T. Bhardwaj, A. Antic, B. Pavan, V. Barone, B.D. Fahlman, Enhanced electrochemical lithium storage by graphene nanoribbons, J. Am. Chem. Soc. 132 (2010) 12556.
[11] G.L. Luque, M.I. Rojas, E.P.M. Leiva, Curvature effect in the longitudinal unzipping carbon nanotubes, J. Solid Electrochem. 17 (2013) 1189.
[12] G. Wang, X. Shen, J. Yao, J. Park, Graphene nanosheets for enhanced lithium storage in lithium ion batteries, Carbon 47 (2009) 2049.
[13] D. Pan, S. Wang, B. Zhao, M. Wu, H. Zhang, Y. Wang, Z. Jiao, Li storage properties of disordered graphene nanosheets, Chem. Mat. 21 (2009) 3136.
[14] W. Lee, S. Suzuki, M. Miyayama, Lithium storage properties of graphene sheets derived from graphite oxides with different oxidation degree, Ceramics Int. 39 (2013) S753.
[15] S.-L. Kuo, W.-R. Liu, C.-P. Kuo, N.-L. Wu, H.-C Wu, Lithium storage in reduced graphene oxides, J. Power Sourc. 244 (2013) 552.
[16] M.E. Stournara, V.B. Shenoy, Enhanced Li capacity at high lithiation potentials in graphene oxide, J. Power Sourc. 196 (2011) 5697.
[17] F. Valencia, A.H. Romero, F. Ancilotto, P.L. Silvestrelli, Lithium adsorption on graphite from density functional theory calculations, J. Phys. Chem. B 110 (2006) 14832.
[18] J.S. Filhol, C. Combelles, R. Yazami, M.L. Doublet, Phase diagrams for systems with low free energy variation: a coupled theory/experiments method applied to Li-graphite, J. Phys. Chem. C 11 (2008), 3982.
[19] K. Persson, Y. Hinuma, Y.S. Meng, A. Van der Ven, G. Ceder, Thermodynamic and kinetic properties of the Li-graphite system from first-principles calculations, Phys. Rev. B 8 (2010), 125416.
[20] E. Lee, K.A. Persson, Li absorption and intercalation in single layer graphene and few layer graphene by first principles, Nano Lett. 12 (2012) 4624.

[21] Y. Liu, V.I. Artyukhov, M. Liu, A.R. Harutyunyan, B.I. Yakobson, Feasibility of lithium storage on graphene and its derivatives, J. Phys. Chem. Lett. 4 (2013) 1737.
[22] P. Giannozzi, et al., QUANTUM ESPRESSO: a modular and open-source software project for quantum simulations of materials, J Phys: Condens. Matter. 21 (2009) 395502.
[23] J.P. Perdew, K.A. Jackson, M.R. Pederson, D.J. Singh, C. Fiolhais, Atoms, molecules, solids, and surfaces: Applications of the generalized gradient approximation for exchange and correlation, Phys Rev B. 46 (1992) 6671.
[24] J.P. Perdew, Y. Wang, Accurate and simple analytic representation of the electron-gas correlation energy, Phys Rev B. 45 (1992) 13244.
[25] D. Vanderbilt, Soft self-consistent pseudopotentials in a generalized eigenvalue formalism, Phys Rev B. 41 (1990) 7892.
[26] M. Liu, A. Kutana, Y. Liu, B.I. Yakobson, First-principles studies of Li nucleation on graphene, J. Phys. Chem. Lett. 5 (2014) 1225.
[27] H.J. Monkhorst, J.D. Pack, Special points for Brillouin-zone integrations, Phys Rev B. 13 (1976) 5188.
[28] L. Liu, L. Wang, J. Gao, J. Zhao, X. Gao, Z. Chen, Amorphous structural models for graphene oxides, Carbon 50 (2012) 1690.
[29] C.B. Robledo, M.I. Rojas, O.R. Cámara, E.P.M. Leiva, First principles studies concerning optimization of hydrogen storage in nanoporous reduced graphite oxide, Int. J. Hydrogen Energy 39 (2014) 4396.
[30] M.K. Aydinol, A.F. Kohan, G. Ceder, K. Cho, J. Joannopoulos, Ab-initio study of lithium intercalation in metal oxides and metal dichalcogenides, Phys Rev B 56 (1997) 1354.
[31] M.K. Aydinol, G. Ceder, First principles prediction of insertion potentials in Li-Mn oxides for secondary Li-batteries, J. Electrochem. Soc. 144 (1997) 3832.
[32] M.D. Levi, D. Aurbach, The mechanism of lithium intercalation in graphite film electrodes in aprotic media. Part 1. High resolution slow scan rate cyclic voltammetric studies and modeling, J. of Electroanal. Chem. 421 (1997) 79.
[33] J.C. Ma, D. Dougherty, The Cation-PI Interaction, Chem. Rev. 97 (1997) 1303.